Is walking a random walk? Evidence for long-range correlations in stride interval of human gait

JEFFREY M. HAUSDORFF, C.-K. PENG, ZVI LADIN, JEANNE Y. WEI, AND ARY L. GOLDBERGER

Charles A. Dana Research Institute of Beth Israel Hospital; Department of Medicine, Beth Israel Hospital; Geriatric Research Education and Clinical Center, Brockton/West Roxbury Department of Veterans Affairs Medical Center; Division on Aging, Harvard Medical School; and Department of Biomedical Engineering, Boston University, Boston, Massachusetts 02215

Hausdorff, Jeffrey M., C.-K. Peng, Zvi Ladin, Jeanne Y. Wei, and Ary L. Goldberger. Is walking a random walk? Evidence for long-range correlations in stride interval of human gait. *J. Appl. Physiol.* 78(1): 349–358, 1995.—Complex fluctuations of unknown origin appear in the normal gait pattern. These fluctuations might be described as being *1*) uncorrelated white noise, *2*) short-range correlations, or *3*) long-range correlations with power-law scaling. To test these possibilities, the stride interval of 10 healthy young men was measured as they walked for 9 min at their usual rate. From these time series, we calculated scaling indexes by using a modified random walk analysis and power spectral analysis. Both indexes indicated the presence of long-range self-similar correlations extending over hundreds of steps; the stride interval at any time depended on the stride interval at remote previous times, and this dependence decayed in a scale-free (fractallike) power-law fashion. These scaling indexes were significantly different from those obtained after random shuffling of the original time series, indicating the importance of the sequential ordering of the stride interval. We demonstrate that conventional models of gait generation fail to reproduce the observed scaling behavior and introduce a new type of central pattern generator model that successfully accounts for the experimentally observed long-range correlations.

fluctuation analysis; locomotion; computer modeling; central pattern generator; fractal

HUMAN GAIT is a complex process. The locomotor system incorporates input from the cerebellum, the motor cortex, and the basal ganglia, as well as feedback from visual, vestibular, and proprioceptive sensors. Under healthy conditions, this multilevel control system produces a remarkably stable walking pattern; the kinetics, kinematics, and muscular activity of gait appear to remain relatively constant from one step to the next, even during unconstrained walking (12, 13, 23, 24, 40). Nevertheless, closer examination reveals fluctuations in the gait pattern, even under stationary conditions (7, 10, 23, 41, 42). We (11) and others (7, 10, 41, 42) have observed considerable "noise" in one of the outputs of the locomotor system, the stride interval, defined as the time between the heel strike of one foot and the next heel strike of the same foot. A representative example of these complex fluctuations is shown in Fig. 1. One possible explanation for these step-to-step variations is that they simply represent uncorrelated (white) noise superimposed on a basically regular process. Alternatively, there could be short-range correlations in the stride interval such that the current value is influenced by only the most recent stride intervals, but over the long term, the fluctuations are random. A third, less intuitive, possibility is that the fluctuations in the stride interval exhibit long-range correlations, as seen in a wide class of scale-free phenomena (6, 14, 17, 28, 34, 38, 43). In this case, the stride interval at any instant would depend on the interval at relatively remote times, and this dependence would decay in a scale-free (fractal-like) power-law fashion.

Defining the nature of these fluctuations is of interest because it may extend our understanding of normal gait mechanisms. Neurophysiological studies in animals have demonstrated that rhythmic movements in general, and locomotor movements in particular, are generated by neural networks often termed central pattern generators (CPGs) (2, 3, 31, 33, 35). These networks have been identified in some invertebrates and vertebrates and may be present in humans as well. If the fluctuations in the stride interval are uncorrelated or represent only short-range correlations, conventional CPG models could readily be modified to account for these dynamics. However, if the fluctuations indicate long-range correlations, a new model is needed to account for this scale-free behavior.

In this study, we sought to quantitatively characterize and model the human stride interval fluctuations. Surprisingly, we observed the presence of long-range correlations in the stride interval that extend over hundreds of steps. This finding motivates the second problem that we address. What might account for the observed long-range correlations? We show that a number of general models of locomotor generation fail to account for this behavior and describe a novel correlated CPG model that simulates the observed scaling behavior.

METHODS

Subjects

Ten young healthy men with no history of any neuromuscular disorders participated in this study. Mean age was 26

0161-7567/95 $3.00

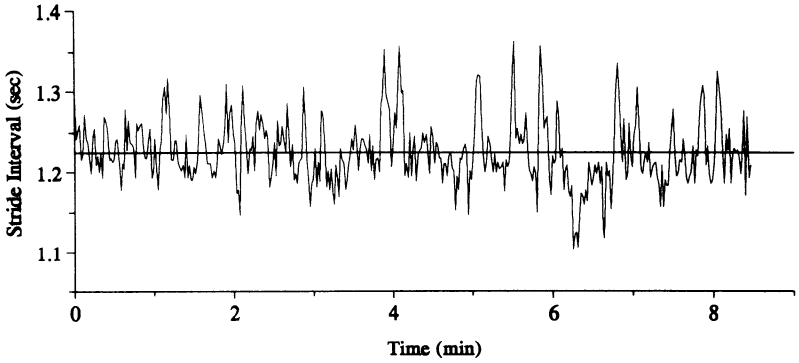

FIG. 1. Stride interval time series of healthy subject during walk with constant conditions. Even though stride interval is fairly constant, it fluctuates about its mean (solid line) in an apparently unpredictable manner. Note that compared with mean value of stride interval, fluctuations are small. SD of fluctuations, 0.04 s, is only 3% of mean value of stride interval, 1.23 s.

yr (range 20–30 yr). Height of the subjects was 1.8 ± 0.1 (SD) m, and weight was 72.2 ± 9.4 kg. All subjects provided informed written consent.

Measurement of Stride Interval

Subjects were instructed to walk continuously on level ground around a 130-m-long approximately circular path at their self-determined usual rate for ~9 min. To measure the stride interval, ultrathin force-sensitive switches were taped beneath one shoe. The data were recorded on an ambulatory recorder, as previously described (11). Subsequently, the recorded gait signal was digitized at the maximal sampling rate of the playback machine (416 Hz real time), and the time between heel strikes was automatically computed.

Analysis of Stride Interval Dynamics

To analyze the dynamics of the stride interval, two scaling indexes that distinguish among white noise, brown noise, and fluctuations with short-range or long-range correlations were calculated from each subject's time series. These indexes were based on two methods: detrended fluctuation analysis (DFA) and power spectral analysis.

DFA. DFA (1, 27) is a modification of classic root-mean square analysis of a random walk (22, 37) and has two important advantages over other scaling analyses: it reduces noise effects and, because the DFA process removes local trends, it is relatively unaffected by any nonstationarities. Briefly, the stride interval time series (of total length N) was first integrated

$$y(k) = \sum_{i=1}^{k} [\mathrm{I}(i) - \mathrm{I}_{\mathrm{avg}}]$$

where $\mathrm{I}(i)$ is the ith stride interval and $\mathrm{I}_{\mathrm{avg}}$ is the average stride interval. Next the integrated time series was divided into boxes of equal length (n). In each box of length n, a least squares line was fit to the data. The y-coordinate of the straight-line segments is denoted by $y_n(k)$. Next, the fluctuation of $y(k)$ about the locally best-fit line was computed for each box of length n and the average fluctuation for that box size [$\mathrm{F}(n)$] was determined

$$\mathrm{F}(n) = \sqrt{\frac{1}{N}\sum_{k=1}^{N} [y(k) - y_n(k)]^2}$$

This computation was repeated over all time scales (box sizes) to provide a relationship between $\mathrm{F}(n)$ and n (i.e., the number of strides in a box or the size of the window of observation). Typically, $\mathrm{F}(n)$ will increase with n. A linear relationship on a double-log graph indicates the presence of scaling. The slope of the line relating log $\mathrm{F}(n)$ to log n determines the scaling exponent α. For a process where the value at one step is completely uncorrelated with any previous values, e.g., white noise, the integrated value, $y(k)$, corresponds to a random walk and therefore $\alpha = 0.5$. If there are short-term correlations, the initial slope may be different from 0.5 but α will approach 0.5 for large window sizes. An $\alpha > 0.5$ and ≤ 1.0 indicates persistent long-range correlations; $\alpha = 1.5$ indicates brown noise, the integration of white noise.[1]

Power spectral analysis. We also calculated a scaling exponent using Fourier analysis. After obtaining the power spectrum of the time series (i.e., the square of the amplitudes of the Fourier spectrum), S(f), we computed the regression line relating log power to log frequency (inverse stride number) from 0.01 to 0.3 (stride number)$^{-1}$. For a scale invariant power-law-correlated process, the negative slope of the regression line is related to another scaling exponent, β, i.e., $\mathrm{S(f)} \approx 1/f^{\beta}$, where f is frequency (6, 17, 34, 38). This scaling exponent characterizes the distribution of the power spectrum. Unlike the DFA method, this analysis is sensitive to noise and nonstationarity effects. For this measure, $\beta = 0$ for white noise, $\beta = 2$ for brown noise, and $\beta = 1$ for $1/f$ noise (5, 29). Theoretically, for data of infinite length, $\alpha = (\beta + 1)/2$ (25).

Surrogate data tests. We applied the method of surrogate data introduced by Theiler et al. (36) to differentiate statistically between long-range scaling and a random process with no long-range correlations. For each subject's time series, 10 surrogate data sets were obtained by randomly shuffling the original time series. Each of the surrogate data sets had the same mean and SD as the original data set, differing only in the sequential ordering of the time series. The mean and SD of the scaling exponent were then calculated for the surrogate data sets and compared with the exponent of the original data set to determine statistical significance. The number of SDs between the original scaling exponent and the mean scaling exponent of the surrogate data sets (σ) was computed. If $\sigma > 3$, i.e., if the scaling exponent of the original data set fell more than 3 SDs away from the exponent of the surrogate data sets, the null hypothesis was rejected and the difference between the original data set and the surrogate data set was considered statistically different.

RESULTS

A representative stride interval time series is shown in Fig. 2*A*. First, note the stability of the stride interval;

[1] Under certain conditions, the DFA exponent α is theoretically equivalent to the Hurst exponent H. However, the Hurst exponent is sensitive to nonstationarities and is operative only in the range $0 \leq H \leq 1$ (6).

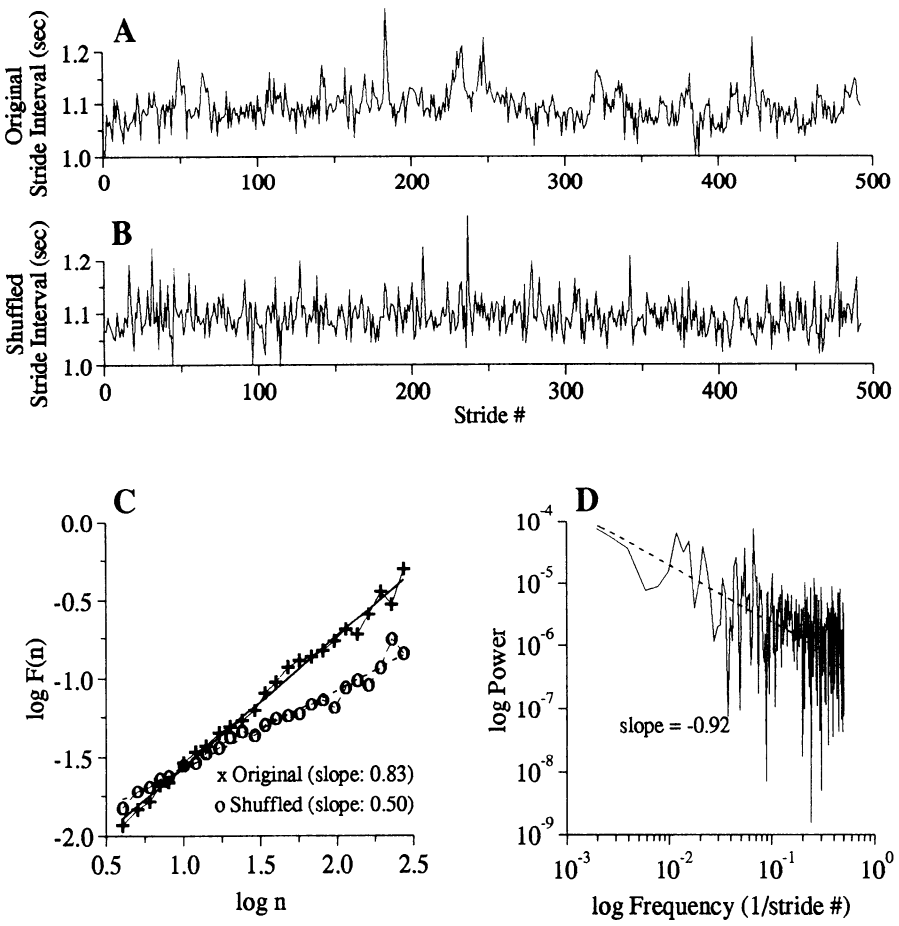

FIG. 2. Representative stride interval time series before (*A*) and after (*B*) shuffling and fluctuation (*C*) and power spectrum analysis (*D*). α, Slope of line relating log of average fluctuation for box size n [log F(n)] to log n, was evaluated by linear regression fit. For all subjects, deviations of data from best-fit line were minimal ($r \geq 0.98$).

during a 9-min walk the coefficient of variation was only 4%. Thus, as in Fig. 1, a good first approximation of the dynamics of the stride interval would be a constant. However, fluctuations occur about the mean. The stride interval varies irregularly with some underlying complex "structure." This structure changes after random shuffling, as seen in Fig. 2*B*, demonstrating that the original structure is a result of the sequential ordering of the stride interval and not a result of the stride interval distribution. Figure 2*C* shows F(n) vs. n plotted on a double-log graph for the original time series and the shuffled time series. The slope of the line relating log F(n) to log n is 0.83 for the original time series and 0.50 after random shuffling. Thus, fluctuations in the stride interval scale as $F(n) \approx n^{0.83}$, exhibiting long-range correlations, whereas the shuffled data set behaves as uncorrelated white noise: $\alpha = 0.50$. Figure 2*D* displays the power spectrum of the original time series. The spectrum is broad band and scales as $1/f^{\beta}$ with $\beta \approx 0.92$. The two scaling exponents are consistent with each other within statistical error due to finite data length (25), and both indicate the presence of long-range correlations.

For the group of 10 subjects, $\alpha = 0.76 \pm 0.11$ (SD) for the original stride interval time series (range 0.56–0.91) and $\alpha = 0.50 \pm 0.03$ after random shuffling (range 0.45–0.55). σ is shown in Fig. 3. For 8 of the 10 subjects, σ was >3, implying that α was significantly different from 0.5. For these eight subjects, the minimum P value was $P < 0.0005$; for four subjects, $P < 10^{-7}$. When we applied the surrogate data test for statistical significance to β the same subjects showed significant differences ($\sigma = 6.9 \pm 3.2$; 8 subjects) between β before (mean $\beta = 0.83 \pm 0.23$; 8 subjects) and after random shuffling (mean $\beta = 0.01 \pm 0.04$; 8 subjects). Thus, for these eight subjects, fluctuations in the stride interval were unlike those obtained from an uncorrelated random walk. Instead, α and β both indicate the presence of long-range correlations.[2]

Modeling of Stride Interval Dynamics

To investigate this scaling phenomenon and the mechanisms that might account for it, we attempted to simulate the experimental results. Several stochastic and deterministic models were tested in search of finding a physiological model that produced long-range correlations comparable to those observed experimentally. After testing several conventional models that

[2] We excluded the possibility that fluctuations due to instrumentation and measurement errors could account for the long-range correlations by *1*) using an electromechanical load cell to periodically activate a foot switch, *2*) computing the differences between the foot switch-based estimates of the period and the actual input period, and *3*) recalculating α from each subject's stride interval time series after adding Gaussian noise equal in magnitude to that of the measurement system noise. This procedure did not significantly change the results. Recalculated α values changed toward 0.5 by <5%.

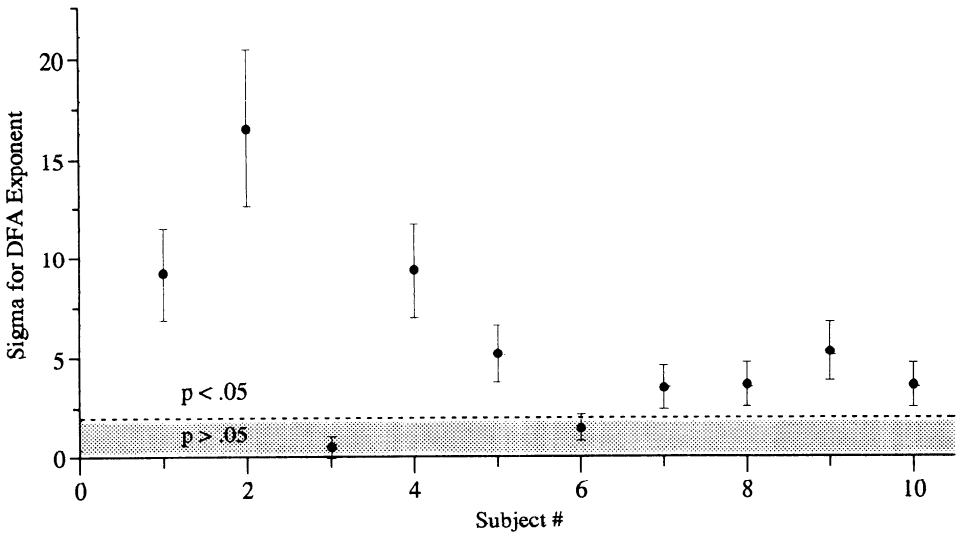

FIG. 3. Testing for statistical significance of α calculated using detrended fluctuation analysis (DFA). For each subject, mean of α from 10 data sets obtained through random shuffling was compared with α of originally ordered time series. Sigma is no. of SDs separating original and shuffled α values. Error bars are computed as described elsewhere (36).

did not account for the long-range correlations, we developed a new model that does reproduce the observed dynamics. Before discussing the successful model, we briefly describe the models that were unsuccessful.

Markov model. For an infinite time series, a Markov process (32) will produce only short-term correlations. However, we wanted to verify that the observed long-range correlations were not a result of spurious detection of apparent long-range correlations of a Markov process with finite length effects. The time series of the experimental data was used to determine a transition probability matrix that defines the probability for the next stride interval for a given previous stride interval (i.e., a 1st-order Markov process). This model did not result in long-range correlations;[3] instead, α was always near 0.5.

Pendulum model of lower leg. We attempted to model the stride interval time series as the outcome of a second-order deterministic system in combination with some stochastic elements. This system could represent simple mass-spring-dashpot models of walking (19, 20) or, as now described, a pendulum model of the lower leg (4). The lower leg was modeled as a pendulum with inertia (leg mass) attached with a damping and spring element (muscles, tendons, ligaments) and torque actuators driving the system. Heel strike was taken as the time the pendulum passed through the origin and the stride interval as the time between heel strikes. For the input to the system, we used a single sinusoid and two sinusoids oscillating at different integer and noninteger frequencies (a simple coupled oscillator). We drove the system with and without additive noise and saturation effects and also added an impulse analogous to that present at heel strike. All of the parameters of the model (inertia, damping, amount of noise) were varied over several decades. From the time series of the model we computed α. Over the entire parameter space, this model was unsuccessful in producing long-range correlations: α was either close to 1.5 (brown noise) or near 0.5 (white noise) but was never between 0.7 and 1.0.

CPG model with noise. Oscillators play a critical role in rhythm generation in many neurophysiologically based CPG models (2, 3, 33, 35). With this in mind, we attempted to determine whether a CPG could produce the observed long-range correlations. A simple oscillator will produce periodic output. We examined whether an oscillator in which the frequency changes randomly (e.g., a "noisy" CPG) could produce dynamics similar to those observed. In this model, a CPG oscillates at a given frequency and the stride interval is defined as the time between cycles. If the frequency is constant, the stride interval will also be constant. However, if the frequency fluctuates from stride to stride, the stride interval will also fluctuate. To generate these fluctuations, we added Gaussian-distributed random noise to the average oscillation frequency at each stride. We also added arbitrary perturbations of the phase of the oscillator randomly during each cycle. The amplitude of each of these two "noise" terms were the two parameters of the model. Simulations over the parameter range showed that a noisy CPG does not produce long-range correlations. Instead, $\alpha \approx 0.50$ over the entire parameter space.

Correlated CPG model. To introduce "memory" into the CPG and produce scale-free behavior, we modified the noisy CPG model. Whereas previously the frequency (mode) of the oscillations could change arbitrarily, we now imposed a rule whereby the CPG mode could change based on some predefined preference where only certain transitions from mode to mode are allowed (possibly with different probabilities). For clarity, we focus here on a simple one-dimensional network CPG model (Fig. 4). Generalizations of this type of model are briefly discussed in the APPENDIX. The one-dimensional model can be viewed as a network where the nodes represent possible frequencies or stable states. Mode transitions will take place from the cur-

[3] We also attempted to simulate the data by superimposing brown and white noise. The brown and white noise might represent changes in the mean stride interval and random fluctuations about the mean, respectively. The amplitude of both noise terms and the probability of changing the mean value were parameters in the model. This model did not produce long-range correlations.

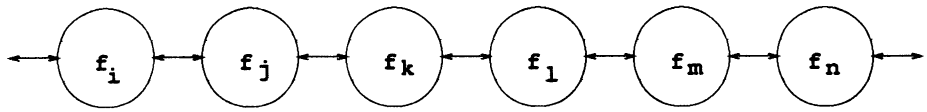

FIG. 4. Schematic portion of 1-dimensional correlated central pattern generator (CPG) model. Circles, fixed allowable modes or frequencies ($f_i, f_j, f_k, \ldots$), values of which were preassigned randomly; lines, allowable transitions among modes. Switching from current mode to next mode takes place randomly, except that transitions at each time step may occur only to 1 of 2 neighboring modes (with equal probability).

rent mode to one of its two neighboring modes with equal probability. The frequency values at each node of the network are assigned randomly, but once determined, they are fixed in time. The net result is that this model, termed the correlated CPG model, differs from the noisy CPG model in a subtle, but crucial, way. The key difference is that oscillator frequencies, once chosen, are now fixed in time. In addition, although the CPG frequency may switch randomly, it switches only to an adjacent mode of (randomly) preassigned frequency. If this restriction is relaxed, i.e., if the network structure is removed such that each mode can switch to any other mode, not just neighboring modes, the outcome is the same as that of the original noisy CPG model. For a time series of an infinite length, α of the correlated CPG model approaches 0.75 (see APPENDIX for a theoretical derivation). However, for finite lengths α may vary about this theoretical value. In fact, for different realizations of the model at the same finite length α will also vary, although the average over many realizations should approach 0.75, approximating the group mean of the experimental stride interval data ($\alpha = 0.76$).

The output of the correlated CPG model for a single realization is shown in Fig. 5. Note the structure in the original time series (Fig. 5*A*) and the lack of structure in the shuffled time series (Fig. 5*B*). The scaling exponent for this simulated time series was $\alpha = 0.91$, indicating long-range correlation. Comparing the output of this realization of the correlated CPG model with 10 surrogate data sets showed that α was significantly different from white noise ($\sigma = 7.1$, $P < 10^{-12}$).

Two stochastic factors are "embedded" in the correlated CPG model, the randomness in the structure of the network (the frequency associated with each mode) and the randomness in the actual mode transitions (choosing the next mode from 1 of 2 neighboring modes). Therefore, we expect that each realization of the correlated CPG model will produce somewhat different scaling behavior even with fixed-model parameters. To investigate whether the differences in α observed experimentally could possibly be due to different realizations of the same underlying model, we simulated 10 realizations of the correlated CPG model using the same parameters in the model. The differences between realizations are in the random assignment of frequencies to each node and in the random switching between neighboring nodes. In Fig. 6, we compare the 10 experimental and 10 model outcomes. Figure 6 (*top*) shows similar results of the DFA analysis, $F(n)$ vs. n, for all 10 subjects (*left*) and for 10 realizations of the correlated CPG model (*right*). α was generally ~0.8 for the model (range 0.71–0.91). Random shuffling of the original time series affected the fluctuation analysis of the experimental and model outputs similarly (Fig. 6, *middle, left* and *right*, respectively). For all cases, $\alpha \approx 0.5$ after random reordering. We plotted the average fluctuation for the 10 subjects and the 10 realizations of the correlated CPG model in Fig. 6 (*bottom, left* and *right*, respectively).[4] For a process with true long-range correlations, spurious effects should be minimized after averaging. Figure 6 demonstrates that this is what occurred for both the experimental and correlated CPG model results. Both data sets show robust scaling behavior (straight line on log-log plot) across two decades.

We used the correlated CPG model to investigate the effects of the finite length of the experimental data sets. Ten realizations of the correlated CPG model were run for time series at lengths of 5,000, 50,000, and 500,000 strides. In all cases, similar results were obtained as those we presented above for the time series length of 500 strides (of course, the region of scaling increased with time series length). For 5,000 strides, α was 0.81 ± 0.05; for 50,000 strides, α was 0.78 ± 0.04; for 500,000 strides, α was 0.77 ± 0.04, approaching the value predicted theoretically.

To gain insight into what would occur physiologically for a longer time series, we recorded data on one additional subject (a 33-yr-old healthy male) as he walked around a 200-m indoor track for 1 h. Figure 7 shows the time series and scaling analysis for this 1-h walk. The time series of 3,500 stride intervals was quite stationary (the stride interval remained between 1.0 and 1.2 s over the entire hour) (Fig. 7*A*). Fluctuation analysis (Fig. 7*C*) showed $\alpha = 0.90$ with scaling evident over two decades, from 3 strides to >300 strides. Ten surrogate data sets produced by random shuffling of this time series (Fig. 7*B*) resulted in $\alpha = 0.50 \pm 0.02$ and showed that the scaling was significantly different from an uncorrelated random walk process ($\sigma = 16.9$, $P < 10^{-20}$).

To learn more about the stability of α and to determine whether differences in α reflect differences in the CPG, we divided the time series of 3,500 strides into seven equal parts (roughly the length of the time series of each of the other 10 subjects) and computed α for each portion. This might be analogous to running the correlated CPG model seven times with the same underlying structure. We found that the variation in α was one-half that observed for the group of 10 subjects

[4] After normalizing each time series by mean and SD, the effect of which is only to shift the log $F(n)$ vs. log n curve up or down, $F(n)$ was averaged over all subjects or realizations. The averaging is justified because normalized histograms of each subject and each model realization were similar.

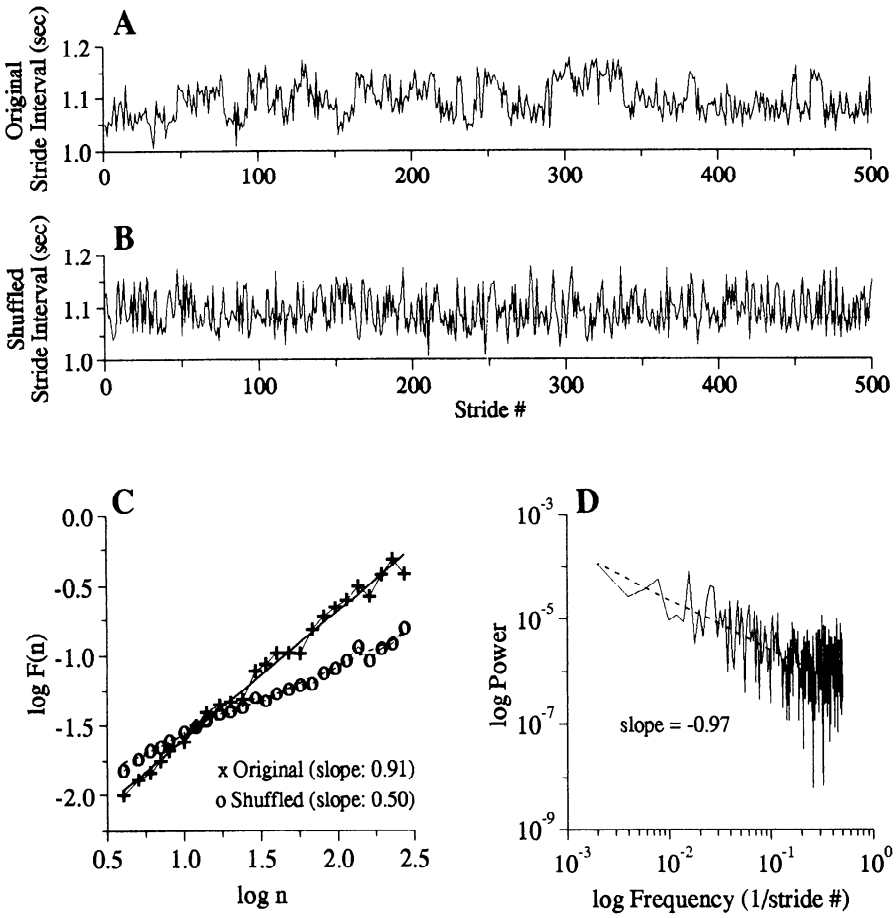

FIG. 5. Correlated CPG model sample results. Representative stride interval time series generated using correlated CPG model before (*A*) and after (*B*) shuffling and fluctuation (*C*) and power spectrum analysis (*D*). In this example, model frequencies were chosen from a uniform distribution, and this resulted in a stride interval ranging from 1 to 1.2 s. Transitions between frequencies were set to change randomly on average once every 5 steps.

(i.e., 10 different network realizations). The model also predicts that variations in α will be much smaller for different realizations of the same underlying network than if the network is changed.

DISCUSSION

This study demonstrates for the first time that the stride interval time series exhibits long-range self-similar correlations. Scaling exponents obtained using two complementary methods, fluctuation analysis and Fourier analysis, both indicate the presence of long-range power-law correlations. With random shuffling of the stride interval, the scaling exponents change significantly to those of an uncorrelated random process. Thus, stride interval fluctuations are not random like white noise, nor are they the outcome of a process with short-term correlations. Instead, the present stride interval is influenced by the interval hundreds of strides earlier, and this scaling occurs in a scale-invariant fractallike manner.

We also introduce a correlated CPG model. This simple model reproduces the dynamics we observed experimentally, dynamics we could not replicate to any degree with numerous other conventional models. The correlated CPG model indicates that the process generating locomotor rhythm possesses a type of "memory" that produces long-term scale-invariant fluctuations. Mathematically, this memory relates to preferences for the transitions between modes. Even though the correlated CPG model does not specify details of the actual underlying physiology, its ability to duplicate the range of results observed experimentally (Fig. 6) suggests that, at the very least, it may be a representative of a class of models that do generate long-range correlations. Future work might explore deterministic models that generate long-range correlations and models that describe the influences of sensory input, the environment, muscle state, and higher center nervous system inputs.[5] Currently, these effects are lumped together as stochastic noise and act as the driving force for the mode switching in our model. However, this representation is arbitrary and is not intended to correspond to specific physiological elements. Nevertheless, the correlated CPG model indicates that the combined effects of all of these influences result in power-law scale-invariant fluctuations.

CPGs, hypothesized to play an important role in rhythmic movements in humans and animals (2, 3, 33, 35), generally produce a periodic or pseudoperiodic output, even in the presence of noise. We found this in

[5] Several relatively simple deterministic systems have been described that produce long-range correlations (8, 9, 16). However, in those cases the correlation properties are due to intermittency (irregular bursting) in the time series (9, 16), and, thus, these systems do not appear to be a relevant model for the fluctuations observed in the stride interval.

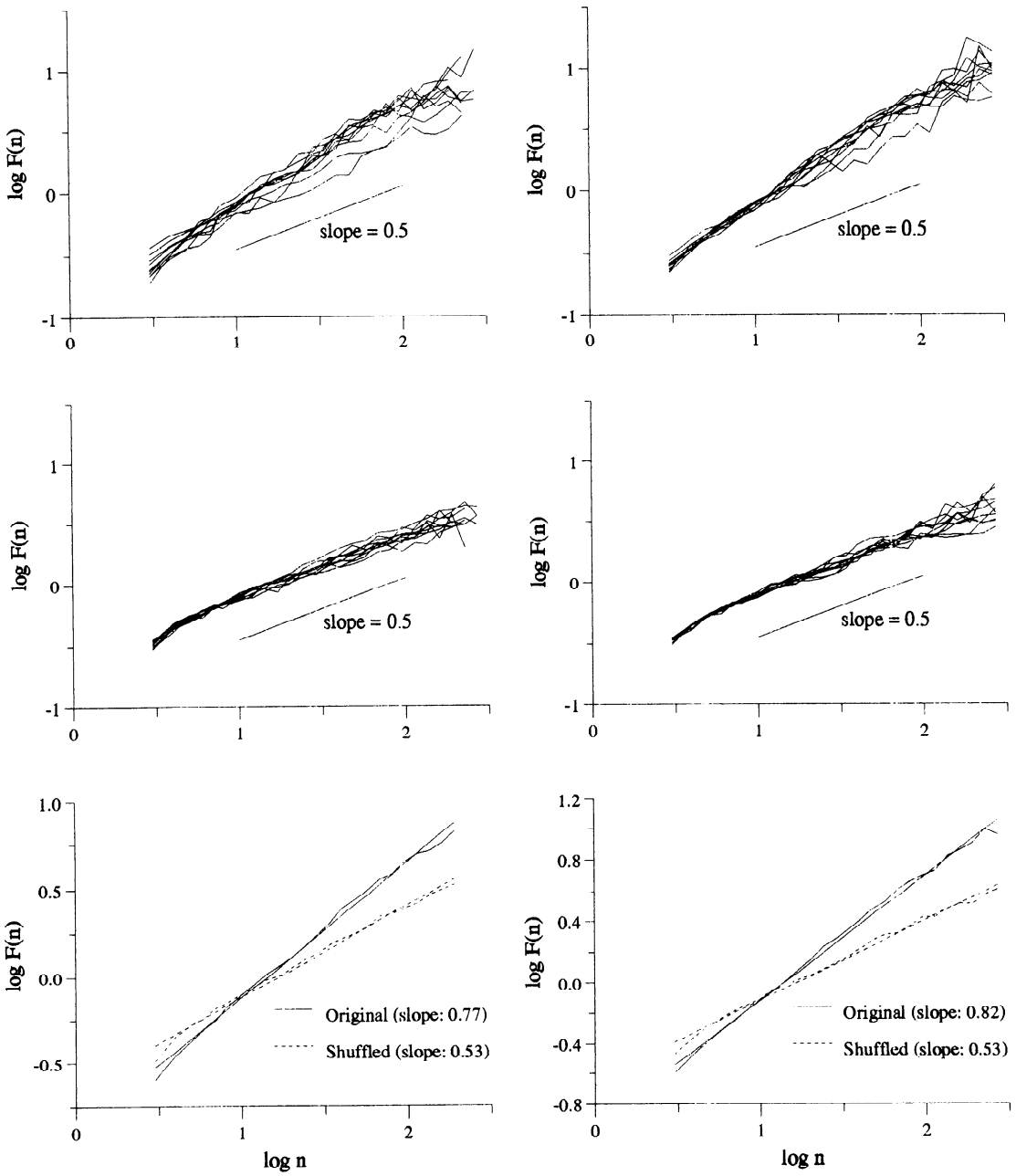

FIG. 6. Group summaries of DFA for experimental and correlated CPG model. *Left*: experimental data. *Right*: data from correlated CPG model. *Top*: DFA of stride interval of 10 subjects and 10 model realizations. *Middle*: DFA of stride interval of 10 subjects and 10 model realizations after random shuffling of original time series. *Bottom*: normalized group averages. Scaling exponent α obtained after averaging of 10 realizations of $F(n)$ vs. n is equivalent to α obtained by averaging individual α values for both experimental data and model. Note that, although theoretical value of α is 0.75 for correlated CPG model, α deviates from this due to finite lengths for time series of 500 strides. Solid and dashed lines for group averages are best-fit lines.

our relatively simple simulations with a second-order system with sinusoids and noise. Taga (35) found similar results using a noise-free, but much more elaborate, hierarchical model of both the CPG and the neuromuscular system under CPG command. When simulating a healthy gait, Taga's model generates a steady-state locomotor pattern with characteristics of a limit cycle. In contrast, when the delay in communication between the CPG and the neuromuscular system increases to 70 ms, the limit cycle disappears and the system never converges to a steady state. Instead, under these conditions, trajectories of phase portraits converge "to an attractor which showed quasi-periodicity" and the state variables wandered within a confined area of the state space (35). Thus, Taga suggests that chaos may be a marker of neurological pathology. In contrast, our findings imply that, under some conditions, long-range correlations and fractallike fluctuations in the locomotor rhythm may actually be a healthy feature of the locomotor system, as observed in other highly complex physiological feedback systems (14, 17, 25, 26, 28, 34).

Further investigation is needed to better understand the mechanisms responsible for and the implications

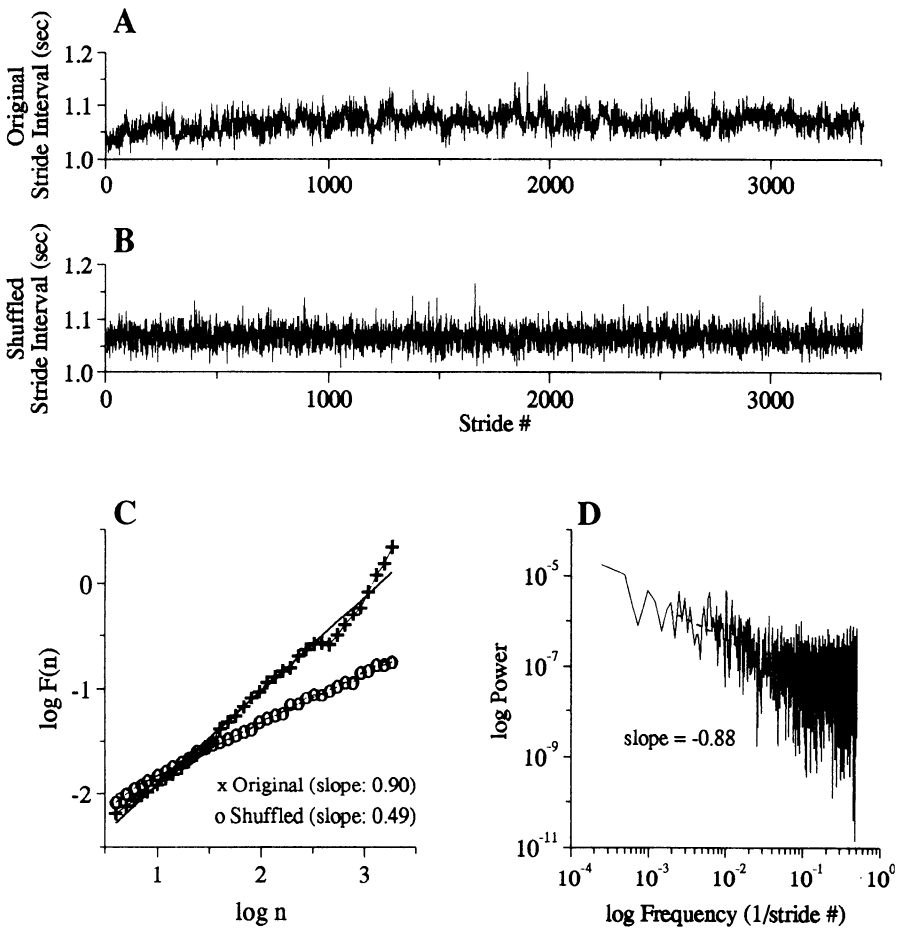

FIG. 7. Stride interval time series during 1-h walk before (*A*) and after (*B*) shuffling and fluctuation (*C*) and power spectrum analysis (*D*).

of long-range correlation in the stride interval. Several questions need to be addressed to better evaluate this phenomenon. When do the long-range correlations in the stride interval exist? What happens at walking rates other than the natural rate and when environmental constraints change? What is the role of the various sensory inputs in generating long-range correlations? Which component(s) of the locomotor system is responsible for the long-range correlations? Processes with long-range correlations are generally more error tolerant and resistant to both internal and environmental perturbations (15, 39); is this also an adaptational feature of the long-range correlations in locomotor control? Do long-range correlations in the stride interval break down with pathology and aging, as observed in other physiological systems (15, 28)?

APPENDIX

We present here a theoretical derivation demonstrating that $\alpha = 0.75$ for the one-dimensional correlated CPG model and discuss the importance of different components of the model.

Let $I(n)$ denote the stride interval of the nth stride. The model is stochastic, and therefore the function I is not definitely determined by the independent variable n. In other words, we obtain different functions $I(n)$ for different observations (realizations). We focus on the statistical expectation value for the autocorrelation function, $C(n_2 - n_1) \equiv \langle I(n_1)I(n_2)\rangle$, of the function $I(n)$. For simplicity, we shift the value of $I(n)$ so that the average value of I is 0. This process does not affect the derivation of α.

In our model, the stride interval is related to the underlying mode (frequency) in which the locomotor system is operating, i.e., $I(n) = u(k)$, where k is an index of CPG mode and the function u maps the frequency of the mode k to the stride interval. The exact functional form of u is not important, but the correlation property of u is

$$\langle u(k)u(k')\rangle_c \propto \delta(k - k') \qquad (A1)$$

where $\langle\ \rangle_c$ denotes an average over all possible configurations of CPG modes. *Equation A1* merely indicates that there is no correlation between different modes, as we described in our model.

For the one-dimensional model, CPG modes are arranged in a connected one-dimensional network (see Fig. 4). The system can hop from one mode (say *mode i*) to its neighboring modes ($i - 1$ and $i + 1$) with equal probability. Therefore, the "hopping" between modes can be viewed as a simple random walk process

$$k(n) = k(n - 1) + \eta(n) = k(0) + \sum_{i=1}^{n} \eta(i) \qquad (A2)$$

where

$$\eta(i) = \begin{cases} +1, \text{ if it hops to the right} \\ -1, \text{ if it hops to the left} \end{cases}$$

and the stochastic variable η satisfies the following correlation

$$\langle \eta(i)\eta(j)\rangle_n = \delta_{i,j} \qquad (A3)$$

where $\langle\ \rangle_n$ denotes the average over all random walk realizations.

Let us calculate the correlation of stride intervals at different times (assuming $n_2 > n_1$)

$$\langle \mathrm{I}(n_1)\mathrm{I}(n_2)\rangle \equiv \langle\langle \mathrm{u}[k(n_1)]\ \mathrm{u}[k(n_2)]\rangle_c\rangle_n \propto \langle \delta[k(n_2) - k(n_1)]\rangle_n$$

using *Eq. A1*

$$= \frac{1}{2\pi}\int \mathrm{d}\omega\ \langle \exp\{i\omega[k(n_2) - k(n_1)]\}\rangle_n$$

$$= \frac{1}{2\pi}\int \mathrm{d}\omega\ \exp\left[-\frac{1}{2}\omega^2\ \langle [k(n_2) - k(n_1)]^2\rangle_n\right] \qquad (A4)$$

where we used the identity $\delta(x) = (1/2\pi)\int \mathrm{d}\omega e^{i\omega x}$ (ω is a dummy variable). Next, we need to calculate the quantity

$$\langle [k(n_2) - k(n_1)]^2\rangle_n = \left\langle \left[\sum_{i=n_1+1}^{n_2} \eta(i)\right]^2 \right\rangle_n \qquad (A5)$$

$$= \sum_{i=n_1+1}^{n_2}\ \sum_{j=n_1+1}^{n_2} \langle \eta(i)\eta(j)\rangle_n = n_2 - n_1$$

where we have used *Eq. A3*. Substituting *Eq. A5* into *Eq. A4*, we obtain

$$\langle \mathrm{I}(n_1)\mathrm{I}(n_2)\rangle \propto \frac{1}{2\pi}\int \mathrm{d}\omega\ \exp\left[-\frac{1}{2}\omega^2\ (n_2 - n_1)\right] \qquad (A6)$$

$$= (n_2 - n_1)^{-1/2}$$

Thus we have shown that the autocorrelation function of stride interval in this correlated CPG model decays like a power law. Because $\mathrm{F}^2(n)$ is the double summation of the autocorrelation function (26, 37), then

$$\mathrm{F}^2(n) \sim \sum_{i-1}^{n}\ \sum_{j-1}^{n} \mathrm{C}(j - i) \sim n^{2-1/2} = n^{3/2}$$

that is

$$\mathrm{F}(n) \sim n^{3/4}$$

or $\alpha = 0.75$. Thus, for a theoretically infinite time series, $\alpha = 0.75$. The above derivation is based on correlation measures. Because the one-dimensional correlated CPG model can be mapped to a well-studied diffusion process, alternative derivations can be found elsewhere (18, 30, 44).

This scaling behavior depends on several factors. If the time series is not infinite, α will deviate from 0.75 due to finite size effects. The scaling behavior also depends on the mode assignment. For example, in our simulation using the correlated CPG model, Gaussian-distributed and uniformly distributed random assignments of the frequencies at each mode produced the same scaling behavior. However, if the frequencies were assigned in some less "complex" manner, the scaling would break down. If the frequencies were assigned in some monotonic fashion, $\alpha \approx 1.5$ (brown noise). The model assumes that there are an infinite number of modes. Actually, however, all that is required is that during the hopping from mode to mode not all modes are explored. For our simulations, this effectively requires only ~10 different modes. If the time series were long enough to explore all of the modes, the scaling behavior would break down at large time scales.

This model can be generalized in two ways. The model can be modified by changing the embedding dimension, and this will produce changes in scaling. For example, for a two-dimensional square-lattice model, $\mathrm{F}(n) \sim (n \cdot \ln n)^{1/2}$, and for dimension ≥ 3, $\alpha \approx 1/2$ because the correlation decays too fast, although it is still power-law decay. Alternatively, the model can be generalized by arranging the modes on an "ultrametric" space. In that case, α will depend on the transition probability between layers and the branching ratio (44). Depending on these values, α can range from 0.5 to 1.0. This case is particularly interesting because under certain conditions ground states of a neural network (CPG modes) can be realized as embedded in ultrametric space (21).

The authors thank J. Mietus, G. B. Moody, J. J. Collins, D. R. Rigney, and H. E. Stanley for valuable discussions and assistance.

This work was supported in part by National Institute on Aging Grants AG-00436, AG-07225, AG-08812, and AG-00294. Additional support was provided by National Heart, Lung, and Blood Institute Grant HL-42172; National Institute on Drug Abuse Grant DA-06306; National Aeronautics and Space Administration Grant NAG9-514; a Boston University Presidential Scholarship (to J. M. Hausdorff); and a National Institute of Mental Health National Research Service Award (to C.-K. Peng). We are also grateful for support from the G. Harold and Leila Y. Mathers Charitable Foundation and the Department of Veterans Affairs.

Address for reprint requests: J. M. Hausdorff, 330 Brookline Ave., Rm. KB-26, Boston, MA 02215.

Received 28 April 1994; accepted in final form 19 September 1994.

REFERENCES

1. **Buldyrev, S. V., A. L. Goldberger, S. Havlin, C.-K. Peng, H. E. Stanley, and M. Simons.** Fractal landscapes and molecular evolution: modeling the myosin heavy chain gene family. *Biophys. J.* 65: 2673–2679, 1993.
2. **Cohen, A. H., S. Rossignol, and S. Grillner.** *Neural Control of Rhythmic Movements in Vertebrates.* New York: Wiley, 1988.
3. **Collins, J. J., and I. Stewart.** Hexapodal gaits and coupled nonlinear oscillator models. *Biol. Cybern.* 68: 287–298, 1993.
4. **Durfee, W. K., and J. M. Hausdorff.** Regulating knee joint position by combining electrical stimulation with a controllable friction brake. *Ann. Biomed. Eng.* 18: 575–596, 1990.
5. **Dutta, P., and P. M. Horn.** Low-frequency fluctuations in solids: 1/f noise. *Rev. Mod. Phys.* 53: 497–516, 1981.
6. **Feder, J.** *Fractals.* New York: Plenum, 1988.
7. **Gabell, A., and U. S. L. Nayak.** The effect of age on variability in gait. *J. Gerontol.* 39: 662–666, 1984.
8. **Geisel, T., J. Nierwetberg, and A. Zacherl.** Accelerated diffusion in Josephson Junctions and related chaotic systems. *Phys. Rev. Lett.* 54: 616–619, 1985.
9. **Grossmann, S., and H. Horner.** Long time correlations in discrete chaotic dynamics. *Z. Phys. B* 60: 79–85, 1985.
10. **Guimares, R. M., and B. Isaacs.** Characteristics of the gait in old people who fall. *Int. Rehab. Med.* 2: 177–180, 1980.
11. **Hausdorff, J. M., D. E. Forman, D. M. Pilgrim, D. R. Rigney, and J. Y. Wei.** A new technique for simultaneous monitoring of electrocardiogram and walking cadence. *Am. J. Cardiol.* 70: 1064–1071, 1992.
12. **Inman, V. T., H. J. Ralston, and F. Todd.** *Human Walking.* Baltimore, MD: Williams & Wilkins, 1981.
13. **Kadaba, M. P., H. K. Ramakrishnan, M. E. Wootten, J. Gainey, G. Gorton, and G. V. B. Cochran.** Repeatibility of kinematic, kinetic and electromyographic data in normal adult gait. *J. Orthop. Res.* 7: 849–860, 1989.
14. **Liebovitch, L. S., and T. I. Toth.** Fractal activity in cell membrane ion channels. *Ann. NY Acad. Sci.* 591: 375–391, 1990.
15. **Lipsitz, L. A., and A. L. Goldberger.** Loss of 'complexity' and

aging. Potential applications of fractals and chaos theory to senescence. *J. Am. Med. Assoc.* 267: 1806–1809, 1993.
16. **Manneville, P.** Intermittency, self-similarity and 1/f spectrum in dissipative dynamical systems. *J. Physique* 41: 1235–1243, 1980.
17. **Marsh, D. J., J. L. Osborn, and A. W. Cowley.** 1/f Fluctuations in arterial pressure and regulation of renal blood flow in dogs. *Am. J. Physiol.* 258 (*Renal Fluid Electrolyte Physiol.* 27): F1394–F1400, 1990.
18. **Matheron, G., and G. de Marsily.** Is transport in porous media always diffusive? A counterexample. *Water Resour. Res.* 16: 901–917, 1980.
19. **McMahon, T. A.** *Muscles, Reflexes, and Locomotion.* Princeton, NJ: Princeton Univ. Press, 1984.
20. **McMahon, T. A., and G. C. Cheng.** The mechanics of running: how does stiffness couple with speed?. *J. Biomech.* 23: 65–78, 1990.
21. **Mezard, M., G. Parisi, and M. A. Virasoro.** *Spin Glass Theory and Beyond.* Singapore: World Scientific, 1987.
22. **Montroll, E. W., and M. F. Shlesinger.** Nonequilibrium phenomena. II. From stochastics to hydrodynamics. In: *The Wonderful World of Random Walks,* edited by J. L. Lebowitz. Amsterdam: North-Holland, 1984, p. 1–121.
23. **Pailhous, J., and M. Bonnard.** Steady-state fluctuations of human walking. *Behav. Brain Res.* 47: 181–190, 1992.
24. **Palta, A. E.** Some characteristics of EMG patterns during locomotion: implications for locomotor control processes. *J. Motor Behav.* 17: 443–461, 1985.
25. **Peng, C.-K., S. V. Buldyrev, A. L. Goldberger, S. Havlin, M. Simons, and H. E. Stanley.** Finite size effects on long-range correlations: implications for analyzing DNA sequences. *Phys. Rev. E* 47: 3730–3733, 1993.
26. **Peng, C.-K., S. V. Buldyrev, A. L. Goldberger, S. Havlin, M. Simons, and H. E. Stanley.** Long-range correlations in nucleotide sequences. *Nature Lond.* 356: 168–170, 1992.
27. **Peng, C.-K., S. V. Buldyrev, S. Havlin, M. Simons, H. E. Stanley, and A. L. Goldberger.** Mosaic organization of DNA nucleotides. *Phys. Rev. E* 49: 1685–1689, 1994.
28. **Peng, C.-K., J. Mietus, J. M. Hausdorff, S. Havlin, H. E. Stanley, and A. L. Goldberger.** Long-range anti-correlations and non-Gaussian behavior of the heartbeat. *Phys. Rev. Lett* 70: 1343–1346, 1993.
29. **Press, W. H.** Flicker noises in astronomy and elsewhere. *Comment. Astrophys.* 7: 103–119, 1978.
30. **Redner, S.** Superdiffusive transport due to random velocity fields. *Physica D* 38: 287–290, 1989.
31. **Schöner, G., and J. A. S. Kelso.** Dynamic pattern generation in behavioral and neural systems. *Science Wash. DC* 239: 1513–1520, 1988.
32. **Shammugan, K. S., and A. M. Breipohl.** *Random Signals: Detection, Estimation and Data Analysis.* New York: Wiley, 1988.
33. **Strogatz, S. H., and I. Stewart.** Coupled oscillators and biological synchronization. *Sci. Am.* 102–109, 1993.
34. **Szeto, H. H., P. Y. Cheng, J. A. Decena, I. Cheng, D.-L. Wu, and G. Dwyer.** Fractal properties in fetal breathing dynamics. *Am. J. Physiol.* 263 (*Regulatory Integrative Comp. Physiol.* 32): R141–R147, 1992.
35. **Taga, G.** Emergence of bipedal locomotion through entrainment among the neuro-musculo-skeletal system and the environment. *Physica D* 75: 190–208, 1994.
36. **Theiler, J., S. Eubank, A. Longtin, B. Galdrikian, and J. D. Farmer.** Testing for nonlinearity in time series: the method of surrogate data. *Physica D* 58: 77–94, 1992.
37. **Wang, M. C., and G. E. Uhlenbeck.** On the theory of the Brownian motion. *Rev. Mod. Phys.* 17: 323–342, 1945.
38. **West, B. J.** *Fracatal Physiology and Chaos in Medicine.* Singapore: World Scientific, 1990.
39. **West, B. J.** Physiology in fractal dimensions: error tolerance. *Ann. Biomed. Eng.* 18: 135–149, 1990.
40. **Winter, D. A.** Kinematic and kinetic patterns in human gait: variability and compensating effects. *Hum. Mov. Sci.* 3: 51–76, 1984.
41. **Yamasaki, M., T. Sasaki, and M. Torii.** Sex difference in the pattern pattern of lower limb movement during treadmill walking. *Eur. J. Appl. Physiol. Occup. Physiol.* 62: 99–103, 1991.
42. **Yamasaki, M., T. Sasaki, S. Tsuzki, and M. Torii.** Stereotyped pattern of lower limb movement during level and grade walking on treadmill. *Ann. Physiol. Anthropol.* 3: 291–296, 1984.
43. **Yeragani, V. K., K. Srinivasan, V. Satyanarayana, R. Pohl, and R. Balon.** Fractal dimension of heart rate time series: an effective measure of autonomic function. *J. Appl. Physiol.* 75: 2429–2438, 1993.
44. **Zumofen, G., J. Klafter, and A. Blumen.** Enhanced diffusion in random velocity fields. *Phys. Rev. A* 42: 4601–4609, 1990.